Nonlinear reversal of the $\mathcal{PT}$-symmetric phase transition in a system of coupled semiconductor microring resonators

Absar U. Hassan,[*] Hossein Hodaei, Mohammad-Ali Miri, Mercedeh Khajavikhan, and Demetrios N. Christodoulides

CREOL/College of Optics and Photonics, University of Central Florida, Orlando, Florida 32816, USA

A system of two coupled semiconductor-based resonators is studied when lasing around an exceptional point. We show that the presence of nonlinear saturation effects can have important ramifications on the transition behavior of this system. In sharp contrast with linear $\mathcal{PT}$-symmetric configurations, nonlinear processes are capable of reversing the order in which the symmetry breaking occurs. Yet, even in the nonlinear regime, the resulting non-Hermitian states still retain the structural form of the corresponding linear eigenvectors expected above and below the phase-transition point. The conclusions of our analysis are in agreement with experimental data.

I. INTRODUCTION

In recent years there has been a growing interest in optical structures based on parity-time ($\mathcal{PT}$) symmetry [1–10]. Along these lines, some intriguing possibilities have been predicted and experimentally demonstrated. These include solitons [11,12], Bloch oscillations, and exceptional lines in $\mathcal{PT}$-symmetric lattices [13–15], unidirectional invisibility [6,16,17], power oscillations [5,6,18], and mode management in laser structures [19–21], to mention a few. In optical realizations, $\mathcal{PT}$ symmetry can be established by judiciously incorporating gain and loss in a given structure. In particular, a necessary condition for this symmetry to hold is that the complex refractive index distribution involved should obey $n(\mathbf{r}) = n^*(-\mathbf{r})$. In other words, the real part of the refractive index profile must be an even function of position, whereas its imaginary counterpart must be odd [1]. Under these latter conditions, an optical system (composed of cavities, waveguides, etc.), can behave in a pseudo-Hermitian fashion provided that the overall attenuation and amplification is appropriately balanced. On the other hand, if the gain-loss contrast exceeds a certain threshold, the $\mathcal{PT}$ symmetry can be spontaneously broken and the spectrum is no longer entirely real [22–24]. This marks the presence of an exceptional point [25–28] or the emergence of a $\mathcal{PT}$-symmetry breaking transition [29–31]. Moreover, a number of studies have suggested that $\mathcal{PT}$-symmetric concepts can also be fruitfully utilized in other settings beyond optics [32–35].

Lately, the phase transitions associated with exceptional points have been effectively utilized to enforce single-mode operation in microring laser resonators [20,36] and pump-induced lasing turn-off [37,38]. In particular, in Ref. [20], it was shown that the selective breaking of $\mathcal{PT}$ symmetry can be exploited to enhance the maximum output power in a desired longitudinal mode. This mode selection scheme is inherently self-adapting and can be used over a broad bandwidth without the need of any other intracavity components. While the mechanism of $\mathcal{PT}$-symmetry breaking is inherently linear, of fundamental interest will be to understand how this process unfolds in the presence of nonlinearity [39,40]. This is imperative given that lasers are by nature nonlinear

devices. In Ref. [39] Lumer *et al.* already indicated that it is possible to reverse the $\mathcal{PT}$ phase transition sequence using the conservative component of a Kerr nonlinearity in a periodic structure. Instead, in this paper we consider the properties of $\mathcal{PT}$-symmetric coupled microring laser cavities in the presence of saturation effects associated with the imaginary part of the nonlinearity.

In what follows we provide a nonlinear model describing the field evolution in two coupled cavities in the presence of saturable gain and loss that is prevalent in semiconductor systems. A dual microring arrangement is studied using a temporal coupled mode formalism [41] when one ring is subjected to optical pumping while its counterpart is kept unpumped. The system is shown to move from the linear broken $\mathcal{PT}$-symmetry domain directly into the nonlinear broken regime. It is further demonstrated that, by increasing the pumping level, the eigenmodes of the system transition into an unbroken pair of $\mathcal{PT}$-symmetric states that exhibit two real eigenvalues. Conversely, if the system starts lasing in an unbroken $\mathcal{PT}$-like phase then it remains there in spite of nonlinear saturation effects. An experimental demonstration of this process, when starting from the broken phase, is presented which is in qualitative agreement with our theoretical results. Finally, we briefly discuss the behavior of this nonlinear system starting from having both microrings equally pumped to eventually blocking the pump from one of them.

II. THEORETICAL MODEL

A schematic of a dual microring arrangement is shown in Fig. 1. Each microring in our system involves a multiple quantum well InGaAsP-InP structure that is embedded in a silica substrate as in Ref. [20]. The top surface of the rings is exposed to air that serves as a cladding. At the operating wavelength of 1.55 μm of this quantum well system, the effective refractive index is $n_e \simeq 3$, while the group index in the waveguide rings is $n_g \simeq 4$. For demonstration purposes here we assume that each cavity supports only a single longitudinal and transverse mode. In general, the dynamics in each cavity in isolation are described by a corresponding set of modal field amplitude equations in conjunction with a carrier evolution equation. Yet, once the carriers attain a steady state, the field
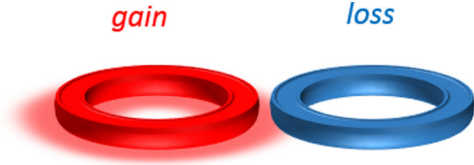
―――――
*absar.hassan@knights.ucf.edu

FIG. 1. (Color online) $\mathcal{PT}$-symmetric arrangement of two coupled microring resonators.

equation can be further simplified according to [42]:

$$\frac{dE}{dt} = \frac{1}{2}\left(\sigma\frac{(p-1)}{1+\varepsilon|E|^2} - \gamma_p\right)(1 - i\alpha_H)E. \qquad (1)$$

Here $p = \tau_e R_p/N_0$ is a pump parameter, where the carrier generation rate $R_p = \eta I/(\hbar\omega d)$ and I, η, d are the pump intensity, the external quantum efficiency, and the depth of each microring, respectively. In addition, τ_e represents the carrier lifetime, N_0 stands for the transparency carrier population density, ω is the frequency of the emitted light, and $\hbar$ is the Planck's constant. The parameter ε is inversely proportional to the saturation intensity $\varepsilon = n_e c\epsilon_0\Gamma a\tau_e/(2\hbar\omega)$ and σ is proportional to the unsaturated loss in the absence of pumping ($\sigma = \Gamma v_g a N_0$). The linear loss γ_p is the inverse of the photon lifetime (τ_p) in the cavity and α_H is the linewidth enhancement factor. Finally, c and ϵ_0 are the speed of light and permittivity in vacuum, respectively, Γ is the confinement factor, v_g represents the group velocity, and a the gain constant [$g = a(N - N_0)$].

Note that in formulating the evolution equations the material response is assumed to be fast compared to carrier and photon lifetimes and hence is considered here to be instantaneous [42]. In our arrangement we assume that the coupling strength between the two rings is strong and hence any frequency detuning that could result from the α_H factor can be ignored. By adopting this latter assumption and denoting the unsaturated gain as $\tilde{g}_0 = \sigma(p - 1)$ and unsaturated loss (at $p = 0$) as $\tilde{f}_0 = \sigma$, we obtain the following two equations describing the dynamics in the aforementioned coupled cavities:

$$\frac{dA_1}{dt} = -\tilde{\gamma}A_1 + \left(\frac{\tilde{g}_0}{1+\varepsilon|A_1|^2}\right)A_1 + i\kappa A_2, \qquad (2a)$$

$$\frac{dA_2}{dt} = -\tilde{\gamma}A_2 - \left(\frac{\tilde{f}_0}{1+\varepsilon|A_2|^2}\right)A_2 + i\kappa A_1. \qquad (2b)$$

In Eq. (2), the modal field amplitudes A_1, A_2 correspond to the pumped and unpumped resonators, respectively, $\tilde{\gamma}$ is the linear loss present in both cavities, and κ is the coupling strength between the resonators. A normalized version of these equations can be easily obtained by adopting the normalized quantities, $a_{1,2} = \sqrt{\varepsilon}A_{1,2}$, $\tau = \kappa t$, $\gamma = \tilde{\gamma}/\kappa$, $f_0 = \tilde{f}_0/\kappa$, and $g_0 = \tilde{g}_0/\kappa$,

$$\dot{a}_1 = -\gamma a_1 + \left(\frac{g_0}{1+|a_1|^2}\right)a_1 + i a_2, \qquad (3a)$$

$$\dot{a}_2 = -\gamma a_2 - \left(\frac{f_0}{1+|a_2|^2}\right)a_2 + i a_1, \qquad (3b)$$

where $\dot{a} = da/d\tau$. In what follows we will study the behavior associated with this system of nonlinear evolution equations.

III. LINEAR DYNAMICAL ANALYSIS

To analyze the response of this arrangement under linear conditions, we assume that the modal field amplitudes are small, i.e., $|a_{1,2}| \sim 0$. Under these assumptions, saturation effects in both the gain and loss mechanisms can be ignored. Hence this regime can be effectively described by a linearized version of Eq. (3), e.g.,

$$\dot{a}_1 = -\gamma a_1 + g_0 a_1 + i a_2, \qquad (4a)$$

$$\dot{a}_2 = -\gamma a_2 - f_0 a_2 + i a_1. \qquad (4b)$$

The eigenvalues of this system, λ, can be directly obtained by adopting the form $(a_1 \quad a_2)^T = (a_{01} \quad a_{02})^T e^{-i\lambda\tau}$, where $a_{01,02}$ are complex constants and T represents a transpose operation. In this respect, two regimes can be identified depending on whether $(g_0 + f_0) \lessgtr 2$. In the first case, where $(g_0 + f_0) < 2$, the modal solutions of Eq. (4) are given by

$$\begin{pmatrix} a_1 \\ a_2 \end{pmatrix} = \begin{pmatrix} 1 \\ \pm e^{\pm i\theta} \end{pmatrix} e^{(\frac{g_0-f_0}{2}-\gamma)\tau} e^{\pm i(\cos\theta)\tau}, \qquad (5)$$

where $\sin\theta = (g_0 + f_0)/2$. We note that the structure of the modal fields closely resembles that expected from an unbroken $\mathcal{PT}$-symmetric coupled arrangement [19]. In particular, the two eigenvectors are by nature nonorthogonal with a phase factor θ that depends on the gain-loss contrast. In addition, a $\mathcal{PT}$-like bifurcation is present around a threshold value given that

$$\cos\theta = \sqrt{1 - \left(\frac{g_0 + f_0}{2}\right)^2}. \qquad (6)$$

If, on the other hand, $(g_0 + f_0) > 2$, the eigenvectors of Eq. (4) are

$$\begin{pmatrix} a_1 \\ a_2 \end{pmatrix} = \begin{pmatrix} 1 \\ i e^{\pm\theta} \end{pmatrix} e^{(\frac{g_0-f_0}{2}-\gamma)\tau} e^{\mp(\sinh\theta)\tau}, \qquad (7)$$

where $\cosh\theta = (g_0 + f_0)/2$. As opposed to those described by Eq. (5), these latter solutions exhibit features of a broken $\mathcal{PT}$-symmetric configuration. In this regime the modal field amplitudes are phase shifted by $\pi/2$ and, moreover, they are unequal.

If the system is operating in the first regime [unbroken $\mathcal{PT}$ symmetry, given by Eq. (5)], then the fields will experience linear amplification as long as the gain is above the total loss in the system, i.e., $g_0 > (2\gamma + f_0) = g_{\text{th}}^{(U)}$. Conversely, in the broken $\mathcal{PT}$-symmetric phase [described by Eq. (7)], growth will occur provided that

$$\left(\frac{g_0 - f_0}{2} - \gamma\right) + \sqrt{\left(\frac{g_0 + f_0}{2}\right)^2 - 1} > 0. \qquad (8)$$

Equation (8) implies that, in this case, the threshold for lasing is dictated by the following condition:

$$g_0 > \frac{1}{\gamma + f_0} + \gamma, \qquad (9)$$

i.e., the gain threshold in this broken symmetry is $g_{\text{th}}^{(B)} = (\gamma + f_0)^{-1} + \gamma$. In view of the above results, one can conclude that the lasing thresholds corresponding to these two regimes (above and below the $\mathcal{PT}$-symmetry breaking point) are
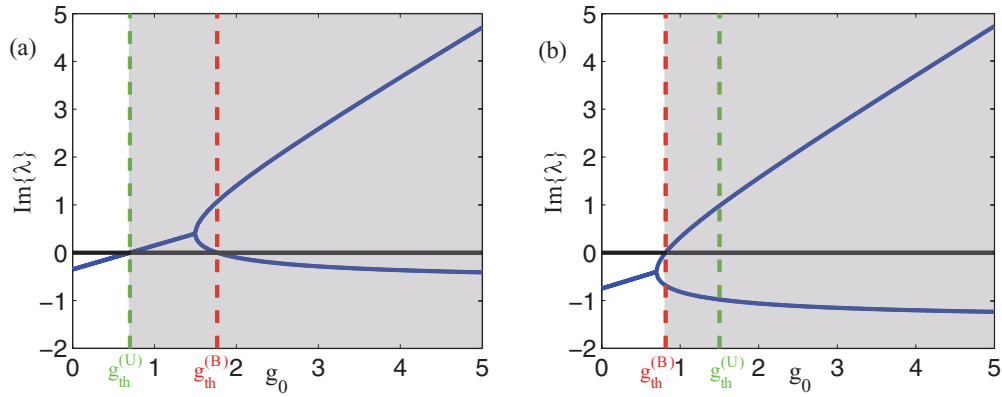
FIG. 2. (Color online) Imaginary components of eigenvalues (blue curves) of the linear system are displayed as the gain level increases. In all cases amplification occurs if $\text{Im}\{\lambda\} > 0$—represented by the gray regions. The broken $\mathcal{PT}$-symmetric phase appears after a bifurcation takes place. The graph in (a) shows that $\text{Im}\{\lambda\} > 0$ before branching occurs, i.e., when $(\gamma + f_0) < 1$, whereas in (b) lasing begins in the broken phase, which takes place when $(\gamma + f_0) > 1$. In both cases the dashed lines indicate the two possible thresholds, where the red line corresponds to the broken phase $[g_{\text{th}}^{(B)} = \gamma + 1/(\gamma + f_0)]$ and the green to the unbroken $(g_{\text{th}}^{(U)} = 2\gamma + f_0)$. The system parameters used here are $\gamma = 0.1$ and (a) $f_0 = 0.5$, (b) $f_0 = 1.3$.

uniquely determined by the parameters, γ and f_0. To compare these thresholds, one has to consider whether $(\gamma + f_0) \gtrless 1$. If, for example, $(\gamma + f_0) > 1$ then the broken phase [Eq. (7)] has a lower threshold and therefore will lase $(g_{\text{th}}^{(B)} < g_{\text{th}}^{(U)})$. Interestingly however, if $(\gamma + f_0) < 1$, the situation is reversed and the unbroken $\mathcal{PT}$ eigenstate, as given by Eq. (5), will experience amplification. The behavior of the system in these two different domains is depicted in Figs. 2(a) and 2(b) for various values of the gain, g_0. Figure 2(b) clearly suggests that for $(\gamma + f_0) > 1$ (i.e., $g_{\text{th}}^{(B)} < g_{\text{th}}^{(U)}$), the lasing threshold is in fact lower than the total loss in the system, $(f_0 + 2\gamma)$. This counterintuitive result is attributed to the coupling process which is in this case relatively slow and therefore does not allow the photon energy to see the entire two-ring system. These two lasing thresholds can be summarized by the following inequality:

$$g_0 > \min\left[\frac{1}{\gamma + f_0} + \gamma, 2\gamma + f_0\right]. \qquad (10)$$

With these preliminary conditions for g_0, needed for lasing, we can now consider the ensuing nonlinear response of this system.

IV. NONLINEAR REGIMES

As the fields in the $\mathcal{PT}$-coupled cavity configuration start to grow, nonlinear saturation effects come into play, as described by Eq. (3). Yet, as we will see, the properties of the linear system not only determine the lasing thresholds, but also provide valuable information as to how this arrangement will respond in the nonlinear regime. More specifically, if $(\gamma + f_0) > 1$, the system will start from a linear broken $\mathcal{PT}$ symmetry and then enter a broken $\mathcal{PT}$-like nonlinear domain. By further increasing the gain, this same arrangement will transition into a nonlinear unbroken $\mathcal{PT}$ phase and will remain there. If, on the other hand, $(\gamma + f_0) < 1$, this structure will lase into an unbroken $\mathcal{PT}$-like domain (whether linear or nonlinear) for all values of the gain g_0 above threshold. It is important to emphasize that, in the first case of $(\gamma + f_0) > 1$,

upon increasing the pump level, a reversal in the order in which symmetry breaking occurs is observed, i.e., the solutions transition from a broken to an unbroken state. The two possible nonlinear phases of lasing are described below along with their corresponding gain parameter ranges.

A. Broken $\mathcal{PT}$

This section is pertinent to the case where lasing takes place in the linear $\mathcal{PT}$-broken regime where $(\gamma + f_0) > 1$. In this scenario, the nonlinear broken-$\mathcal{PT}$ supermodes can be directly obtained by assuming stationary solutions for the field amplitudes that have the form $(a_1 \quad a_2)^T = (a_{01} \quad a_{02})^T$, where $a_{01,02}$ are complex constants. Equation (3) is then reduced to

$$0 = -\gamma a_{01} + \left(\frac{g_0}{1 + |a_{01}|^2}\right)a_{01} + i a_{02}, \qquad (11a)$$

$$0 = -\gamma a_{02} - \left(\frac{f_0}{1 + |a_{02}|^2}\right)a_{02} + i a_{01}. \qquad (11b)$$

These equations clearly suggest that a_{01} and a_{02} are out of phase by $\pi/2$. This in turn allows one to write $a_{02} = i\rho a_{01}$, where $\rho \in \text{Re}^+$ [see Eq. (11b)] represents the modal ratio. From Eq. (11), we readily obtain the following quartic polynomial equation for ρ:

$$\rho^4 - \left(g_0 + \frac{1}{\gamma} - \gamma\right)\rho^3 + \left(\frac{g_0 - f_0}{\gamma} - 2\right)\rho^2$$

$$+ \left(-f_0 + \frac{1}{\gamma} - \gamma\right)\rho + 1 = 0. \qquad (12)$$

In solving Eq. (12), we look for a real root in the interval $[0,1]$ since, from a physical perspective, one expects that under steady-state conditions, the modal field in the lossy ring will be less than that with gain. In addition, one can show that among all four possible roots, that contained in $[0,1]$ happens to be the only stable one. It is important to note that similar to the broken symmetry modes in linear $\mathcal{PT}$ systems, the solution sets in this regime are characterized by an asymmetric
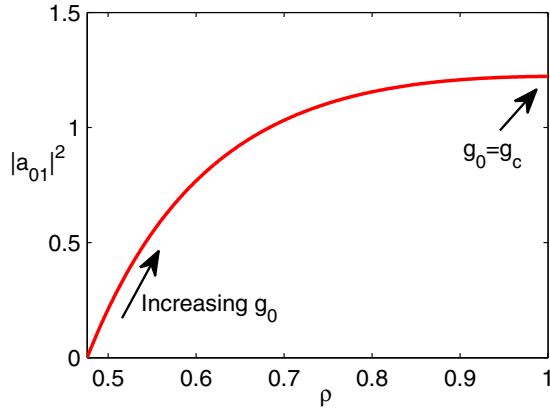
FIG. 3. (Color online) Light intensity in the pumped ring as a function of the modal ratio ρ, as obtained from Eqs. (11) and (12) when $f_0 = 2$ and $\gamma = 0.1$. The linear gain g_0 is varied between $g_{\mathrm{th}}^{(B)} = 0.58$ and $g_c = 2.44$.

distribution of modal fields in the two coupled resonators. For this specific reason, the point $\rho = 1$ is crucial since it marks a $\mathcal{PT}$-preserving transition. The critical gain value (g_c) where this transition occurs is found to be

$$g_c = f_0 \frac{(1 + \gamma)}{(1 - \gamma)}. \quad (13)$$

Note that this critical gain value is smaller than the lasing threshold needed for the linear unbroken phase, $g_{\mathrm{th}}^{(U)}$, that is possible in the parameter range $(\gamma + f_0) < 1$. Hence this nonlinear broken $\mathcal{PT}$ phase only arises once lasing begins in the linear broken $\mathcal{PT}$ phase which only occurs when $(\gamma + f_0) > 1$, where we also have $g_c > g_{\mathrm{th}}^{(B)}$. To demonstrate the energy occupancy in the two cavities, we vary the value of g_0 in the range $g_{\mathrm{th}}^{(B)} < g_0 < g_c$. Figure 3 depicts these results for $\gamma = 0.1$ and $f_0 = 2$.

As it can be seen in Fig. 3, higher values of g_0 not only result in higher steady state intensities in the resonators but also lead to an increased ratio (ρ) that eventually becomes unity. As previously mentioned, an unequal distribution of the fields in the two rings, along with a phase difference of $\pi/2$ clearly indicates that the solution sets in this regime have broken $\mathcal{PT}$-like forms as in Eq. (7). Moreover, there is no frequency shift associated with the resonance of the ring system—another indicator of a broken $\mathcal{PT}$ symmetry.

Remarkably, if one considers linear $\mathcal{PT}$-symmetric dimers, it is well known that the difference between the field intensities in the two components of the dimer becomes larger as we increase the gain-loss contrast beyond the spontaneous symmetry breaking point, indicated by the term $e^{\pm\theta}$ in Eq. (7). However, in the nonlinear case, higher pumping levels (larger values of gain) eventually lead the system to the symmetric phase, at $\rho = 1$. Figure 4 shows the time evolution of the modal intensities as a function of τ after solving Eq. (3) for $g_0 = 1$ and $g_0 = 2.3$. This latter figure demonstrates that higher pump levels eventually enforce a transition towards an unbroken phase where the modal ratio is unity. To summarize, the relevant gain range for solutions within this regime is $g_{\mathrm{th}}^{(B)} < g_0 < g_c$, provided that $(\gamma + f_0) > 1$.
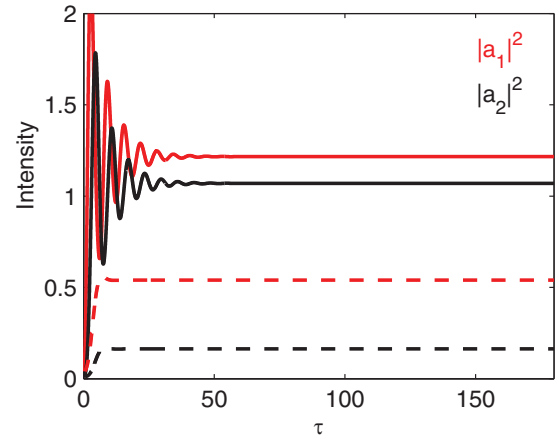

FIG. 4. (Color online) Unequal distribution of steady state intensities (broken symmetry) in the rings with gain (red) and loss (black) is shown. The curves are obtained after numerically integrating Eq. (3) for $\gamma = 0.1$ and $f_0 = 2$. Dashed lines represent the solution for $g_0 = 1$ and solid lines are obtained for $g_0 = 2.3$. A higher gain naturally results in higher intensities but, at the same time, the intensity contrast between the two resonators decreases.

B. Unbroken $\mathcal{PT}$

Before we discuss in detail the properties associated with the nonlinear unbroken $\mathcal{PT}$ symmetry, we note that the results of this section are applicable in both regimes, i.e., $(\gamma + f_0) \gtrless 1$. To obtain the nonlinear eigenmodes in the $\mathcal{PT}$-symmetric phase, we now assume time harmonic solutions, $(a_1 \quad a_2)^T = (a_{01} \quad a_{02})^T e^{i\lambda\tau}$, where $\lambda \in \mathrm{Re}$. In this case, Eq. (3) leads to the following relations:

$$i\lambda a_{01} = -\gamma a_{01} + \left(\frac{g_0}{1 + |a_{01}|^2}\right) a_{01} + i a_{02}, \quad (14a)$$

$$i\lambda a_{02} = -\gamma a_{02} - \left(\frac{f_0}{1 + |a_{02}|^2}\right) a_{02} + i a_{01}. \quad (14b)$$

Using the representation $g_s = g_0/(1 + |a_{01}|^2)$ for the saturated gain and $f_s = f_0/(1 + |a_{02}|^2)$ for the saturated loss and assuming that $a_{01,02} \neq 0$, we get a quadratic equation for the eigenvalues,

$$\lambda^2 - i(2\gamma + f_s - g_s)\lambda - (\gamma^2 + \gamma(f_s - g_s) - g_s f_s + 1) = 0. \quad (15)$$

Given that λ is real, it is necessary that

$$\left(\frac{g_s}{2\gamma}\right) - \left(\frac{f_s}{2\gamma}\right) = 1. \quad (16)$$

This last relation is directly satisfied through the parametric representation $g_s = 2\gamma \cosh^2(\eta)$ and $f_s = 2\gamma \sinh^2(\eta)$, where η is a positive real quantity. In this respect we arrive at the following relations for the intensities:

$$|a_{01}|^2 = \frac{g_0}{2\gamma \cosh^2(\eta)} - 1, \quad (17)$$

$$|a_{02}|^2 = \frac{f_0}{2\gamma \sinh^2(\eta)} - 1. \quad (18)$$

The eigenvalue Eq. (15) now readily reduces to $\lambda^2 = 1 - \gamma^2 \cosh^2(2\eta)$, in which case $\lambda_{1,2} = \pm \cos\theta_{\mathrm{nl}}$, provided that

$\gamma \cosh(2\eta) = \sin\theta_{\mathrm{nl}}$. Here θ_{nl} represents a nonlinear phase shift ranging between 0 and $\pi/2$. Moreover, after dividing Eq. (14a) by a_{01} and Eq. (14b) by a_{02}, upon subtraction we obtain

$$2i \sin\theta_{\mathrm{nl}} = (\rho - \rho^{-1})\cos\phi + i(\rho + \rho^{-1})\sin\phi, \quad (19)$$

where $a_{02} = \rho\, e^{i\phi} a_{01}$. Equation (19) can be solved for the real and imaginary parts, from where one finds that, $\rho = \pm 1$ and $\phi = \pm\theta_{\mathrm{nl}}$, which clearly suggests that $|a_{01}|^2 = |a_{02}|^2$. This is only possible as long as [by considering Eqs. (17) and (18)],

$$\tanh(\eta) = \sqrt{\frac{f_0}{g_0}}, \quad (20)$$

i.e., $g_0 > f_0$. The eigenvalue expression in Eq. (15) now simplifies to

$$\lambda^2 = 1 - \gamma^2 \left(\frac{g_0 + f_0}{g_0 - f_0}\right)^2. \quad (21)$$

Equation (21) directly indicates that real eigenvalues are only possible if $g_0 \geqslant f_0(1 + \gamma)/(1 - \gamma)$, which is equivalent to $g_0 \geqslant g_c$, corroborating the earlier findings in Sec. IV A. In other words the gain level has to be above this critical value, a necessary condition for observing solution sets in this regime. The unfolding of the nonlinear eigenvalues as a function of the gain level is shown in Fig. 5. From these results, one can then determine the unbroken nonlinear $\mathcal{PT}$-symmetric eigenvectors, e.g.,

$$\begin{pmatrix} a_1 \\ a_2 \end{pmatrix} = \sqrt{\left(\frac{g_0 - f_0}{2\gamma} - 1\right)} \begin{pmatrix} 1 \\ \pm e^{\pm i\theta_{\mathrm{nl}}} \end{pmatrix} e^{\pm i(\cos\theta_{\mathrm{nl}})\tau}, \quad (22)$$

where $\sin\theta_{\mathrm{nl}} = \gamma(g_0 + f_0)/(g_0 - f_0)$. When Eqs. (17) and (18) are used in conjunction with Eq. (20), they provide another restriction on the value of g_0 since $|a_i|^2 > 0$. More specifically, the restriction is given by $g_0 \geqslant (2\gamma + f_0) = g_{\mathrm{th}}^{(\mathrm{U})}$. Hence the
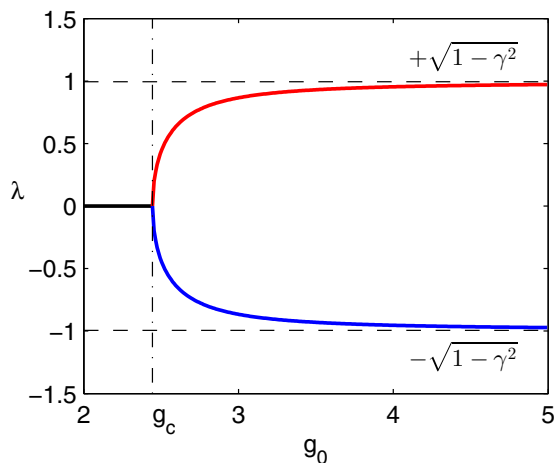

FIG. 5. (Color online) Eigenvalues of the nonlinear system exhibit a square-root bifurcation when entering the unbroken symmetry regime. The region $g_0 < g_c$ represents broken symmetry where the eigenvalues are degenerate. The parameter values used here are $\gamma = 0.1$ and $f_0 = 2$. The eigenvalues $\lambda_\pm$ approach the asymptotes $\pm\sqrt{1 - \gamma^2}$ for large values of g_0.

complete range of g_0 for this solution to exist is

$$g_0 \geqslant g_c \cap g_0 \geqslant g_{\mathrm{th}}^{(\mathrm{U})}. \quad (23)$$

It should be noted here that under the condition $(\gamma + f_0) > 1$, i.e., when lasing begins in the broken $\mathcal{PT}$ phase, once the gain level exceeds g_c, both conditions in Eq. (23) are satisfied, and the steady state now assumes the nonlinear unbroken form of Eq. (22). This confirms the aforementioned reversal of $\mathcal{PT}$-symmetric phase transition due to the nonlinearity. However, if $(\gamma + f_0) < 1$, where lasing begins in the linear unbroken $\mathcal{PT}$ phase, the lasing threshold $g_{\mathrm{th}}^{(\mathrm{U})}$ is greater than g_c, which immediately implies that once lasing begins, the system will eventually attain the nonlinear unbroken $\mathcal{PT}$-symmetric steady state solutions, described by Eq. (22).

The time evolution of intensities in the two coupled resonators can be studied by numerically solving Eq. (3). These results are displayed in Fig. 6(a). Notice that, in this domain, the modal amplitudes eventually become equal (irrespective of initial conditions), an indication of a nonlinear unbroken $\mathcal{PT}$ symmetry. The analytical expressions in Eq. (22) suggest that the system admits two fixed point solutions, $\lambda_{1,2} = \pm\cos\theta_{\mathrm{nl}}$. The choice between the two depends upon the initial conditions provided. An effective method of deducing which initial conditions correspond to which of the two attractors is to project the initial vector onto the two nonlinear eigenmodes.

The projection operation has to be carried out in a $\mathcal{PT}$-symmetric sense [43], i.e., respecting biorthogonality, which implies that for two vectors $\Phi_1 = (\phi_{1x} \quad \phi_{1y})^T$ and $\Phi_2 = (\phi_{2x} \quad \phi_{2y})^T$,

$$\langle\Phi_1|\Phi_2\rangle = (\phi_{1y}^* \quad \phi_{1x}^*)\begin{pmatrix} \phi_{2x} \\ \phi_{2y} \end{pmatrix}. \quad (24)$$

By considering the eigenvectors in Eqs. (5) or (22), and by letting $v_1 = (1 \quad e^{i\theta})^T$ and $v_2 = (1 \quad -e^{-i\theta})^T$, any initial state $v_0 = (a_{01} \quad a_{02})^T$ can then be projected. Absolute values of the complex coefficients $c_1 = \langle v_0|v_1\rangle$ and $c_2 = \langle v_0|v_2\rangle$ associated with these eigenvectors can then be obtained and are given by

$$|c_1|^2 = |a_{01}|^2 + |a_{02}|^2 + 2|a_{01}||a_{02}|\cos(\Delta\phi_0 - \theta), \quad (25)$$

$$|c_2|^2 = |a_{01}|^2 + |a_{02}|^2 - 2|a_{01}||a_{02}|\cos(\Delta\phi_0 + \theta), \quad (26)$$

where $\Delta\phi_0 = \phi_{a_{01}} - \phi_{a_{02}}$ is the initial phase difference between a_{01} and a_{02}. As we will see, the eigenvector with the larger initial amplitude will eventually dominate.

The eigenvalue for the vector v_1 is $\lambda_1 = \cos\theta$, which implies a counterclockwise rotation in the complex plane. Note that this corresponds to the low frequency supermode since the fast variations in the field leading to Eq. (1) were assumed to be of the form $e^{-i\omega_0 t}$, where ω_0 is the resonance frequency of each individual resonator. Similarly, the other eigenvalue $\lambda_2 = -\cos\theta$ corresponds to its high frequency counterpart.

For counterclockwise rotation, one requires that $|c_1|^2 > |c_2|^2$ and vice versa for clockwise rotation. Since $\cos\theta > 0$ for $\theta = [0,\pi/2]$, these conditions can be reduced to (i) $\Delta\phi_0 \leqslant \pi/2$, where the low frequency supermode survives, and (ii) $\Delta\phi_0 > \pi/2$, favoring its high frequency counterpart. As an example, let $g_0 = 2.25$, $f_0 = 1$, and $\gamma = 0.1$ that satisfy
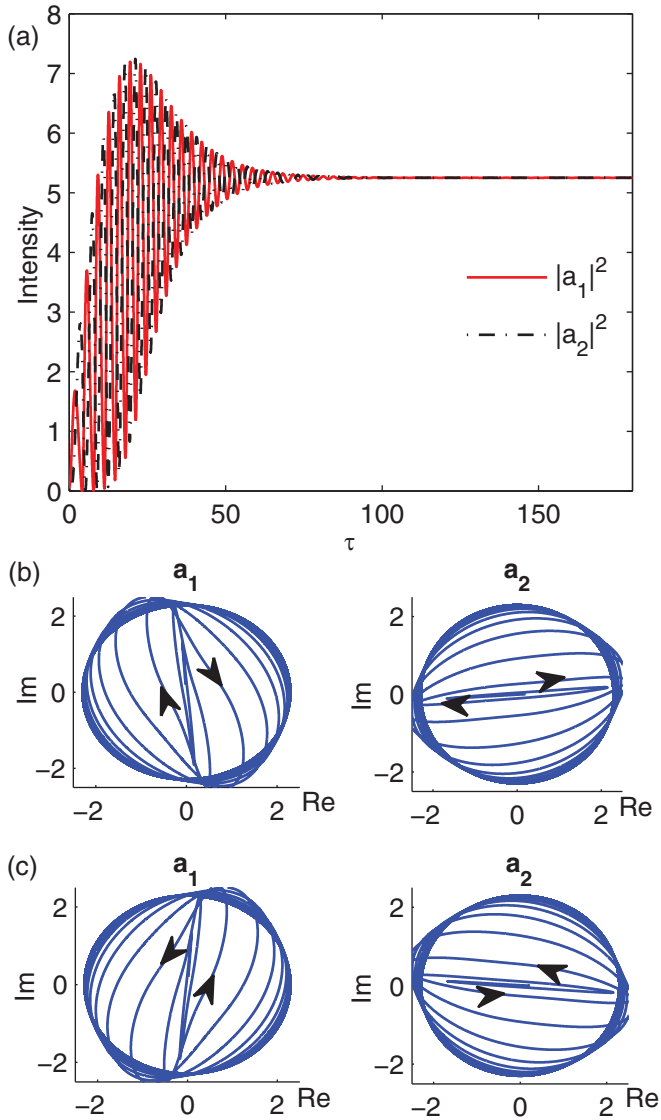
FIG. 6. (Color online) (a) Intensity evolution in the two rings is plotted against time τ, when $g_0 = 2.25$, $f_0 = 1$, and $\gamma = 0.1$. Trajectory of the modal fields when (b) $\Delta\phi = \pi/2 + 0.1$—clockwise rotation and (c) $\Delta\phi = \pi/2 - 0.1$—counterclockwise rotation.

the conditions in Eq. (23). We now consider two cases for the phase difference in the initial values a_{01} and a_{02}. Figure 6(b) shows the field evolution when the initial amplitudes in the two rings are equal, $|a_{01}| = |a_{02}| = 0.2$, but the phase difference is $\Delta\phi_0 = \pi/2 + 0.1$ and (c) shows the same case when $\Delta\phi_0 = \pi/2 - 0.1$. The intensity evolution with time for these two cases happens to be identical and is depicted in Fig. 6(a). The initial exponential growth is evident and the intensities finally saturate to a common value as given by Eq. (22). We note that in an actual experiment, both eigenmodes will be excited from noise and hence the spectrum will involve two lines at $\pm\kappa\cos(\theta_{\mathrm{nl}})$ around ω_0.

V. GENERAL SYSTEM BEHAVIOR

Based on the results of the previous sections, it can be established that, in the steady state, the form of the nonlinear
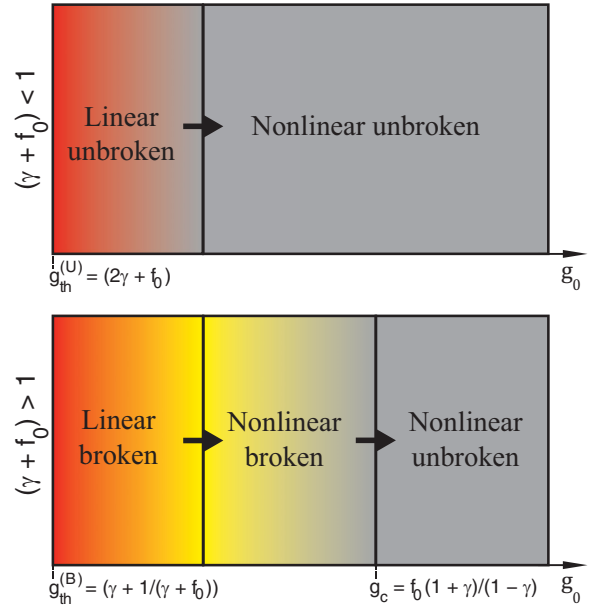

FIG. 7. (Color online) System response as a function of gain in two different parameter regimes is schematically shown. In the upper half, where $(\gamma + f_0) < 1$, the system is always in an unbroken $\mathcal{PT}$ phase. In the lower half, however, where $(\gamma + f_0) > 1$, the configuration first transitions from a linear broken to a nonlinear broken phase and then eventually enters the nonlinear unbroken domain when g_0 exceeds g_c.

solutions is predetermined by the system parameters, specifically by the normalized values of unsaturated absorption (f_0) and linear loss (γ). In the coupled ring resonator arrangement, as the pumping level is increased (as g_0 increases), there are two possible scenarios for the system behavior. If $(\gamma + f_0) < 1$, lasing begins in the linear unbroken $\mathcal{PT}$-symmetric domain [Eq. (5)] and then moves into the nonlinear unbroken $\mathcal{PT}$-symmetric regime where the field intensities are equal in both rings albeit with a phase difference, according to Eq. (22). If, on the other hand, $(\gamma + f_0) > 1$, lasing starts in the linear broken $\mathcal{PT}$-symmetric domain [Eq. (7)] and then transitions into the nonlinear broken $\mathcal{PT}$-symmetric phase where the distribution of field strengths in the two coupled resonators is asymmetric and a phase difference of $\pi/2$ exists between them, as established in Sec. IV A. At even higher gain levels, interestingly, a phase transition occurs from the broken domain into the nonlinear unbroken $\mathcal{PT}$ domain when $g_0 > g_c$. The two scenarios are summarized in Fig. 7, where the nonlinear reversal of a $\mathcal{PT}$-symmetric phase transition (broken to unbroken) is displayed in the lower half. It should be noted that the lasing thresholds in these two cases are different and both paths eventually end up in the unbroken $\mathcal{PT}$-like phase as the gain is increased.

VI. EXPERIMENTAL RESULTS

To experimentally verify our findings, we used lithographic techniques to fabricate sets of coupled microring resonators comprised of six InGaAsP (indium-gallium-arsenide-phosphide) quantum wells embedded in InP, capable of
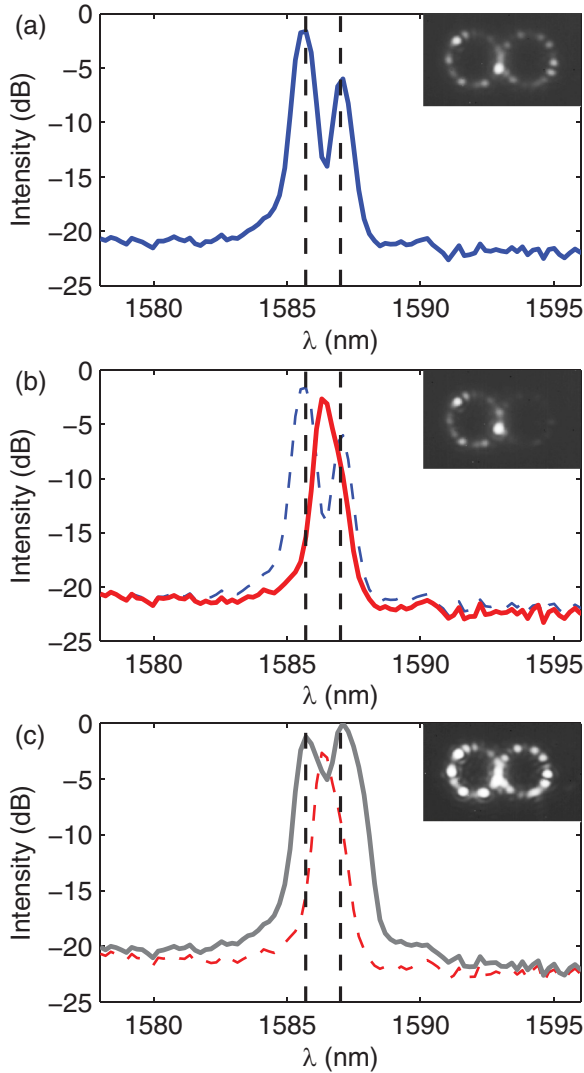
FIG. 8. (Color online) Emitted spectrum from (a) uniformly pumped coupled microrings with the pump power of 0.4 mW (b) $\mathcal{PT}$-symmetric structure when 0.4 mW of pump power reaches the active ring (c) $\mathcal{PT}$-symmetric structure when the active ring is subjected to 0.8 mW pump power. The insets depict mode profiles of the different scenarios, recorded by the scattering from the surface of the rings. Dashed vertical lines are used to compare the locations of resonances.

providing amplification in the wavelength range 1350–1600 nm. A detailed description of the fabrication process can be found in Ref. [20]. The rings in our experiments have an outer radius of 10 μm, a width of 500 nm, and a height of 210 nm. Such dimensions are deliberately chosen so that the rings support a single transverse mode and to also favor the TE polarization. At first, the two coupled resonators were evenly illuminated using a circular pump beam with a diameter of 80 μm. The intensity distribution and spectrum of the modes in the microrings are monitored using a CCD camera and a spectrometer, respectively. Figure 8(a) shows the spectrum of the two active rings when both are exposed to a peak pump power of 0.4 mW (15 ns pulses with a repetition rate of 290 kHz). Under these conditions, coupling-induced mode splitting can

clearly be seen. Next, a knife edge is used to selectively withhold the pump power from one of the rings, hence establishing a $\mathcal{PT}$-symmetric gain-loss microring arrangement. Figure 8(b) illustrates the lasing spectrum of this $\mathcal{PT}$ system. As expected, lasing occurs exclusively in the active cavity and the frequency of the resonance shifts to the center of the supermode peaks. In other words, the system starts lasing in the broken $\mathcal{PT}$ phase as predicted in Sec. IV A. Next, the pump power illuminating the active ring is increased by a factor of two while again keeping the lossy ring in the dark. The emission spectrum of the $\mathcal{PT}$ arrangement subjected to such a high pump power is depicted in Fig. 8(c). In agreement with our theoretical predictions (Sec. IV B), the $\mathcal{PT}$ symmetry of the combined structure is now restored due to a saturation of nonlinearities. In this regime, both resonators are again contributing equally to lasing and as a result two supermode wavelength peaks are now present in the measured spectrum. Our experimental results confirm the fact that nonlinear processes are indeed capable of reversing the order in which the symmetry breaking occurs.

The discussions in earlier sections are also applicable to the findings in Ref. [20]. In that work, lasing was observed when both microrings were at first equally illuminated [in a way similar to Fig. 8(a)], in which case the system was positioned in the unbroken $\mathcal{PT}$-symmetry phase. This behavior is in agreement with our theoretical results presented in Sec. IV B provided that one sets $f_0 = -g_0$. In this case, η is purely imaginary and $\theta_{\mathrm{nl}} = 0$, and hence the normalized eigenvalues are $\lambda_{1,2} = \pm 1$, i.e., the mode splitting is twice the coupling between the two cavities—resembling that in standard Hermitian systems. On the other hand, by removing the pump from one of the rings, saturable losses are introduced since now f_0 is positive. In this scenario, Eq. (23) is no longer satisfied and as a result the system enters the broken $\mathcal{PT}$ phase, in agreement with the observed behavior in Ref. [20].

VII. CONCLUSIONS

In conclusion, we have shown that a nonlinear dimer of two coupled microring laser resonators can transition from a nonlinear broken $\mathcal{PT}$-symmetric phase into an unbroken $\mathcal{PT}$ domain provided that lasing was initiated in a broken mode. This surprising result is a by-product of nonlinear saturation that is capable of reestablishing the $\mathcal{PT}$-symmetric phase, something that is not possible in the linear domain. On the other hand, if lasing initially occurs in an unbroken mode, the system always remains in the unbroken phase even under nonlinear conditions. In all cases, in spite of the presence of nonlinearities, the eigenmodes of this arrangement retain features associated with linear eigenvectors in $\mathcal{PT}$-symmetric configurations.

[1] K. G. Makris, R. El-Ganainy, D. N. Christodoulides, and Z. H. Musslimani, Phys. Rev. Lett. **100**, 103904 (2008); R. El-Ganainy, K. G. Makris, D. N. Christodoulides, and Z. H. Musslimani, Opt. Lett. **32**, 2632 (2007).

[2] A. Guo, G. J. Salamo, D. Duchesne, R. Morandotti, M. Volatier-Ravat, V. Aimez, G. A. Siviloglou, and D. N. Christodoulides, Phys. Rev. Lett. **103**, 093902 (2009).

[3] S. Klaiman, U. Günther, and N. Moiseyev, Phys. Rev. Lett. **101**, 080402 (2008).

[4] S. Longhi, Phys. Rev. A **82**, 031801 (2010).

[5] C. E. Rüter, K. G. Makris, R. El-Ganainy, D. N. Christodoulides, M. Segev, and D. Kip, Nat. Phys. **6**, 192 (2010).

[6] A. Regensburger, C. Bersch, M.-A. Miri, G. Onishchukov, D. N. Christodoulides, and U. Peschel, Nature (London) **488**, 167 (2012).

[7] E.-M. Graefe and H. F. Jones, Phys. Rev. A **84**, 013818 (2011).

[8] T. Kottos, Nat. Phys. **6**, 166 (2010).

[9] S. V. Suchkov, S. V. Dmitriev, B. A. Malomed, and Y. S. Kivshar, Phys. Rev. A **85**, 033825 (2012).

[10] H. Ramezani, T. Kottos, R. El-Ganainy, and D. N. Christodoulides, Phys. Rev. A **82**, 043803 (2010).

[11] Z. H. Musslimani, K. G. Makris, R. El-Ganainy, and D. N. Christodoulides, Phys. Rev. Lett. **100**, 030402 (2008).

[12] M. Wimmer, A. Regensburger, M.-A. Miri, C. Bersch, D. N. Christodoulides, and U. Peschel, Nat. Commun. **6**, 7782 (2015).

[13] S. Longhi, Phys. Rev. Lett. **103**, 123601 (2009).

[14] K. G. Makris, R. El-Ganainy, D. N. Christodoulides, and Z. H. Musslimani, Phys. Rev. A **81**, 063807 (2010).

[15] B. Zhen, C. W. Hsu, Y. Igarashi, L. Lu, I. Kaminer, A. Pick, S.-L. Chua, J. D. Joannopoulos, and M. Soljacic, Nature (London) **525**, 354 (2015).

[16] Z. Lin, H. Ramezani, T. Eichelkraut, T. Kottos, H. Cao, and D. N. Christodoulides, Phys. Rev. Lett. **106**, 213901 (2011).

[17] L. Feng, Y.-L. Xu, W. S. Fegadolli, M.-H. Lu, J. E. Oliveira, V. R. Almeida, Y.-F. Chen, and A. Scherer, Nat. Mater. **12**, 108 (2013).

[18] K. G. Makris, L. Ge, and H. E. Türeci, Phys. Rev. X **4**, 041044 (2014).

[19] M.-A. Miri, P. LiKamWa, and D. N. Christodoulides, Opt. Lett. **37**, 764 (2012).

[20] H. Hodaei, M.-A. Miri, M. Heinrich, D. N. Christodoulides, and M. Khajavikhan, Science **346**, 975 (2014).

[21] H. Hodaei, M. A. Miri, A. U. Hassan, W. E. Hayenga, M. Heinrich, D. N. Christodoulides, and M. Khajavikhan, Opt. Lett. **40**, 4955 (2015).

[22] C. M. Bender and S. Boettcher, Phys. Rev. Lett. **80**, 5243 (1998).

[23] M. Znojil, Phys. Lett. A **285**, 7 (2001).

[24] Z. Ahmed, Phys. Lett. A **282**, 343 (2001).

[25] T. Kato, *Perturbation Theory for Linear Operators* (Springer, Berlin, 1966).

[26] M. V. Berry, Czech. J. Phys. **54**, 1039 (2004).

[27] W. D. Heiss, J. Phys. A **45**, 444016 (2012).

[28] R. El-Ganainy, M. Khajavikhan, and L. Ge, Phys. Rev. A **90**, 013802 (2014).

[29] L. Chang, X. Jiang, S. Hua, C. Yang, J. Wen, L. Jiang, G. Li, G. Wang, and M. Xiao, Nat. Photon. **8**, 524 (2014).

[30] B. Peng, Ş. K. Özdemir, F. Lei, F. Monifi, M. Gianfreda, G. L. Long, S. Fan, F. Nori, C. M. Bender, and L. Yang, Nat. Phys. **10**, 394 (2014).

[31] Y. D. Chong, L. Ge, and A. D. Stone, Phys. Rev. Lett. **106**, 093902 (2011).

[32] J. Schindler, A. Li, M. C. Zheng, F. M. Ellis, and T. Kottos, Phys. Rev. A **84**, 040101 (2011).

[33] R. Fleury, D. Sounas, and A. Alù, Nat. Commun. **6**, 5905 (2015).

[34] J. M. Lee, T. Kottos, and B. Shapiro, Phys. Rev. B **91**, 094416 (2015).

[35] A. Basiri, I. Vitebskiy, and T. Kottos, Phys. Rev. A **91**, 063843 (2015).

[36] L. Feng, Z. J. Wong, R.-M. Ma, Y. Wang, and X. Zhang, Science **346**, 972 (2014).

[37] M. Liertzer, L. Ge, A. Cerjan, A. D. Stone, H. E. Türeci, and S. Rotter, Phys. Rev. Lett. **108**, 173901 (2012).

[38] M. Brandstetter, M. Liertzer, C. Deutsch, P. Klang, J. Schöberl, H. Türeci, G. Strasser, K. Unterrainer, and S. Rotter, Nat. Commun. **5**, 4034 (2014).

[39] Y. Lumer, Y. Plotnik, M. C. Rechtsman, and M. Segev, Phys. Rev. Lett. **111**, 263901 (2013).

[40] I. V. Barashenkov and M. Gianfreda, J. Phys. A **47**, 282001 (2014); I. V. Barashenkov, D. E. Pelinovsky, and P. Dubard, *ibid.* **48**, 325201 (2015).

[41] B. E. Little, S. T. Chu, H. A. Haus, J. Foresi, and J.-P. Laine, J. Lightwave Technol. **15**, 998 (1997).

[42] G. Agrawal and N. Dutta, *Long-wavelength Semiconductor Lasers* (Van Nostrand Reinhold, New York, 1986).

[43] C. M. Bender, D. C. Brody, and H. F. Jones, Phys. Rev. Lett. **89**, 270401 (2002).